

https://doi.org/10.1130/G51257.1

Manuscript received 1 August 2022 Revised manuscript received 23 March 2023 Manuscript accepted 2 June 2023

Published online 15 June 2023

© 2023 Geological Society of America. For permission to copy, contact editing@geosociety.org

# Three-dimensional glacial isostatic adjustment modeling reconciles conflicting geographic trends in North American marine isotope stage 5a relative sea level observations

Schmitty B. Thompson<sup>1,\*</sup>, Jessica R. Creveling<sup>1</sup>, Konstantin Latychev<sup>2</sup>, and Jerry X. Mitrovica<sup>2</sup>
<sup>1</sup>College of Earth, Ocean, and Atmospheric Sciences, Oregon State University, 101 SW 26<sup>th</sup> Street, Corvallis, Oregon 97331, USA
<sup>2</sup>Department of Earth and Planetary Sciences, Harvard University, 20 Oxford Street, Cambridge, Massachusetts 02138, USA

#### **ABSTRACT**

Glacial isostatic adjustment (GIA) simulations using earth models that vary viscoelastic structure with depth alone cannot simultaneously fit geographic trends in the elevation of marine isotope stage (MIS) 5a relative sea level (RSL) indicators across continental North America and the Caribbean and yield conflicting estimates of global mean sea level (GMSL). We present simulations with a GIA model that incorporates three-dimensional (3-D) variation in North American viscoelastic earth structure constructed by combining high-resolution seismic tomographic imaging with a new method for mapping this imaging into lateral variations in lithospheric thickness and mantle viscosity. We pair this earth model with a global ice history based on updated constraints on ice volume and geometry. The GIA prediction provides the first simultaneous reconciliation of MIS 5a North American and Caribbean RSL highstands and strengthens arguments that MIS 5a peak GMSL reached values close to that of the Last Interglacial. This result highlights the necessity of incorporating realistic 3-D earth structure into GIA predictions with continent-scale RSL data sets.

# INTRODUCTION

Reconstructions of peak global mean sea level (GMSL) during past warm intervals serve to calibrate ice sheet sensitivity to past climate and contextualize future change (Dutton et al., 2015). One method to estimate GMSL is to fit sea level predictions from numerical glacial isostatic adjustment (GIA) models to compilations of relative sea level (RSL) indicator elevations corrected for tectonics (Lambeck and Chappell, 2001). GIA encompasses gravitational, rotational, and deformational effects that drive spatially variable RSL change during glacialinterglacial cycles (Mitrovica and Milne, 2003). The representation of the viscoelastic earth in GIA models is key to accurate predictions of this variability. GIA studies generally adopt a onedimensional (1-D), radially varying earth model, yet this approach ignores the complex thermo-

S.B. Thompson **b** https://orcid.org/0009-0007

\*thomschm@oregonstate.edu

chemical mantle structure inferred from seismic tomography (Schaeffer and Lebedev, 2014).

Numerically intensive methods incorporating laterally varying (three-dimensional; 3-D) earth structure into GIA models (Wu and van der Wal, 2003; Zhong et al., 2003; Latychev et al., 2005) underpin studies of the sensitivity of RSL predictions to earth structure (Austermann et al., 2013; Nield et al., 2018; Powell et al., 2021), reappraisals of enigmatic inferences of 1-D earth structure based on RSL data (Kuchar et al., 2019), and efforts to improve fits to deglacial RSL indicators (Li et al., 2018, 2022; Clark et al., 2019). Here we extend the temporal scope of 3-D GIA studies to analyze a comprehensive, continental-scale observational RSL data set for prior to the Last Glacial Maximum (LGM). We focus on marine isotope stage (MIS) 5a at ca. 80 ka, the younger of two orbital precession-paced warm intervals that interrupted global cooling out of the Last Interglacial (LIG; Cutler et al., 2003).

No attempt to estimate MIS 5a peak GMSL with a single 1-D earth model has reconciled RSL highstand elevations across continental North America and the Caribbean (Creveling

et al., 2017). While the 1-D GIA analyses of Potter and Lambeck (2003) and Simms et al. (2015) reconciled trends in MIS 5a RSL highstands from the U.S. Atlantic states to the Caribbean and along the U.S. and Mexico Pacific coast, respectively, Creveling et al. (2017) demonstrated that these 1-D earth models were unable to fit RSL data from the opposite North American coast and postulated that this misfit arises from lateral variation in viscoelastic earth structure between the active Pacific and passive Atlantic margins (Burdick et al., 2008). Using distinct 1-D earth models to best fit RSL data from these two geographic data sets and RSL indicators from the far field of LGM ice sheets, Creveling et al. (2017) inferred that MIS 5a GMSL peaked at  $-8.5 \pm 4.6$  m relative to the present day; an alternate analysis performed on a restricted data set with a robust chronology yielded an estimate of  $-10.5 \pm 5.5$  m. These GMSL predictions differed from the estimates of -28 m and -15.2 m by Potter and Lambeck (2003) and Simms et al. (2015), respectively. Here we present new MIS 5a GIA predictions using a high-resolution 3-D viscoelastic earth model (Richards et al., 2020; Hoggard et al., 2020; Austermann et al., 2021). We demonstrate that introducing complex earth structure in GIA models can, for the first time, simultaneously reconcile continent-scale trends in MIS 5a RSL elevations spanning the North American Pacific and Atlantic-Caribbean coasts.

## **METHODS**

We compute spatially variable MIS 5a RSL change using a finite volume formulation of GIA that supports 3-D variations in Maxwell viscoelastic structure (Latychev et al., 2005). The global numerical grid has  $20 \times 10^6$  nodes with a spatial discretization varying from 15 km at earth's surface to  $\sim 50$  km at the core-mantle

CITATION: Thompson, S.B., et al., 2023, Three-dimensional glacial isostatic adjustment modeling reconciles conflicting geographic trends in North American marine isotope stage 5a relative sea level observations: Geology, v. XX, p. , https://doi.org/10.1130/G51257.1

J.R. Creveling **b** https://orcid.org/0000-0002

K. Latychev https://orcid.org/0000-0002

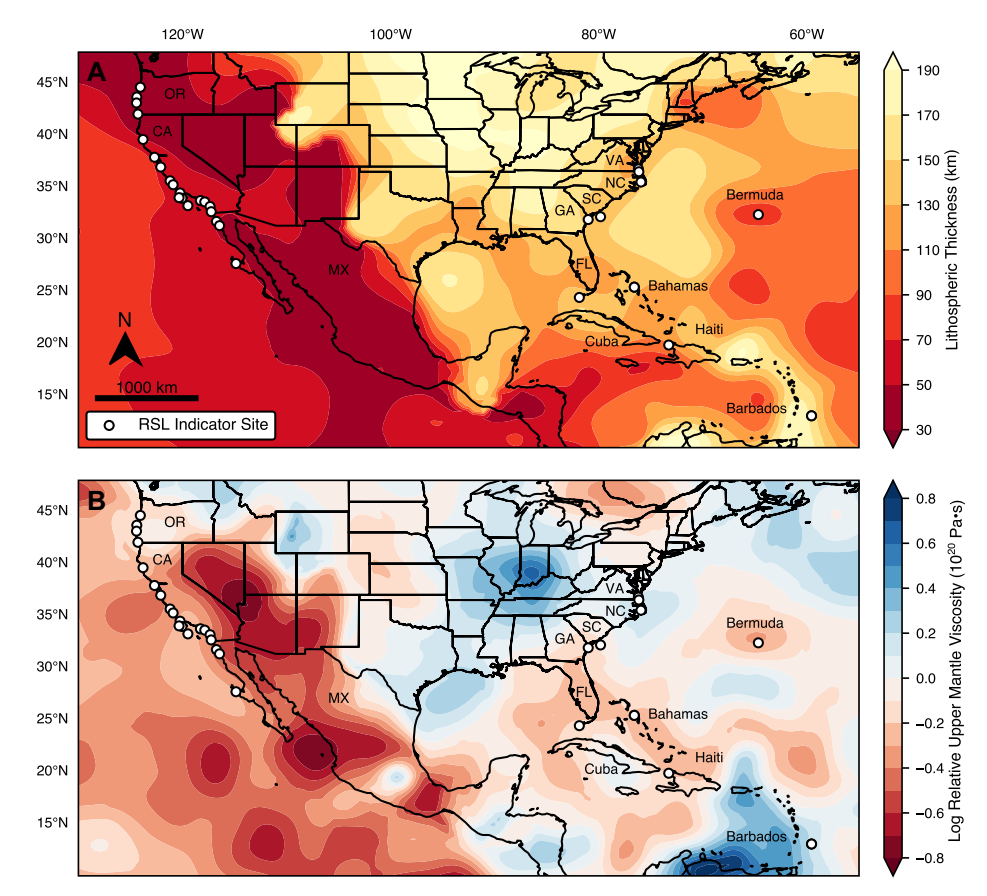


Figure 1. Three-dimensional viscoelastic earth model adopted in glacial isostatic adjustment calculations, showing geographic variation in lithospheric thickness (A) and logarithm of volumetric mean upper mantle viscosity relative to the background one-dimensional earth model (B). Open circles indicate marine isotope stage 5a relative sea level (RSL) indicator sites (Table S1 [see text footnote 1]). OR—Oregon; CA—California; MX—Mexico; VA—Virginia; NC, SC—North and South Carolina; GA—Georgia; FL—Florida.

boundary. We computed gravitationally self-consistent sea level changes using a method that accurately tracks shoreline migration and RSL feedbacks from load-induced perturbations to earth's rotation (Kendall et al., 2005; Mitrovica et al., 2005). This requires model inputs for earth structure and ice geometry.

Following Austermann et al. (2021), our 3-D earth model adopts lateral variations in mantle viscosity and elastic lithospheric thickness derived by Richards et al. (2020) and Hoggard et al. (2020), who combined shear wave seismic tomographic models based on the dense USArray seismic station network across North America (Schaeffer and Lebedev, 2014) with laboratory measurements of mantle materials under high pressure, seismic attenuation measurements, and constraints on the thermal state of the lithosphere and mantle. The model has a global mean lithospheric thickness of 80 km and spherically averaged upper and lower mantle viscosities of  $5 \times 10^{20}$  Pa·s and  $5 \times 10^{21}$  Pa·s, respectively, consistent with GIA inferences from Lambeck et al., (2014) and Lau et al. (2016). We refer to this as the background 1-D model.

The structure of the 3-D model shows heterogeneity across the North American Pacific

and Atlantic-Caribbean coasts (Fig. 1). The Pacific coast has an elastic lithospheric thickness of 40–50 km (Fig. 1A) and a shallow upper mantle viscosity of  $\sim\!10^{20}$  Pa·s (Fig. 1B;  $\sim\!5\times$  lower than the background 1-D value) that reflects the active margin (James et al., 2000). Lithospheric thickness along the Atlantic seaboard is 130–150 km, with a north-to-south gradient in depth-averaged upper mantle viscosity (relatively constant north of North Carolina, dropping from 7  $\times$  10 $^{20}$  Pa·s to 2.5  $\times$  10 $^{20}$  Pa·s from North Carolina to Florida, and rising toward Cuba). The average viscosity over this area is near the background 1-D value of 5  $\times$  10 $^{20}$  Pa·s.

We adopt the PC2T ice history across the last glacial cycle (Pico et al., 2017). Our version of PC2T is identical to ICE-6G from the LGM to present day (ca. 26–0 ka; Peltier et al., 2015) but differs significantly prior to the LGM across MISs 3, 5a, and 5c. For PC2T, MIS 5a GMSL peaks at -13~m, consistent with 1-D GIA modeling of Creveling et al. (2017). The ice history from MIS 6 to LGM is adopted from Austermann et al. (2021).

We fit the 3-D GIA predictions to a compilation of MIS 5a RSL indicators (Table S1

in the Supplemental Material<sup>1</sup>) along the North American Pacific coast from Newport, Oregon (44.6°N), to Turtle Bay, Mexico (27.7°N), and along the North American Atlantic coast and Caribbean from Virginia Beach, Virginia (36.8°N) to Barbados (13.1°N). We adopt RSL highstand elevations as reported in primary publications and correct these for tectonics following the method of Creveling et al. (2015). For each site, we combine the MIS 5e highstand predicted by the 3-D model with a suite of excess ice melt scenarios (GMSL range 1-7 m; Dyer et al., 2021) that source melt (1) evenly across the LIG, (2) only at the start of the LIG, or (3) at the start of the LIG with later attenuated melt, and estimate the tectonic uplift rate by subtracting these totals from the observed elevation. MIS 5a tectonic uplift-corrected highstand elevations maintain or increase elevation moving south along the Pacific coast and decrease markedly in elevation moving south from the Atlantic coast to the Caribbean (Fig. 2).

#### RESULTS

To illustrate GIA physics, we first consider a prediction of MIS 5a peak RSL across North America and the Caribbean using the background 1-D model (Fig. 3B). The peak GMSL of PC2T (-13 m) was subtracted from the map to isolate GIA effects. On both coastlines from  $\sim 35^{\circ}$ N to  $45^{\circ}$ N, peak values of  $\sim 12$  m above present sea level mark the peripheral bulge of the Laurentide and Cordilleran Ice Sheets, which is predicted in this simulation at a higher elevation at present than at MIS 5a (Creveling et al., 2017). Both coasts show similar north-south trends tapering to near zero at Baja California (Mexico) and Barbados. Most MIS 5a RSL indicators fall within or southward of the outer flank of the peripheral bulge predicted by this 1-D earth model.

The 3-D GIA prediction (Fig. 3A) differs significantly from the 1-D simulation (Figs. 3B and 3C). The model's high viscosity and thicker lithosphere along latitudinal band  $\sim\!40^{\circ}N$  east of  $\sim\!100^{\circ}W$  (Fig. 1B) raise the region's peak GIA signal by  $\sim\!12\text{--}24$  m by slowing the post-LGM subsidence of the peripheral bulge. This increases the elevation difference between present day and MIS 5a and steepens the predicted RSL gradient southward relative to the 1-D prediction. In contrast, the thinner Pacific coast lithosphere and the weaker upper mantle of the 3-D model (Fig. 1) reduce the predicted RSL elevation by as much as  $\sim\!9$  m by increasing the post-LGM

<sup>&#</sup>x27;Supplemental Material. Table S1: North American and Caribbean Marine Isotope Stage 5a and 5e sea level indicator data. Figures S1 and S2 on the sensitivity of model predictions to ice margin geometry and plate boundary thickness. Please visit https://doi.org/10.1130/GEOL.S.23304176 to access the supplemental material, and contact editing@geosociety.org with any questions.

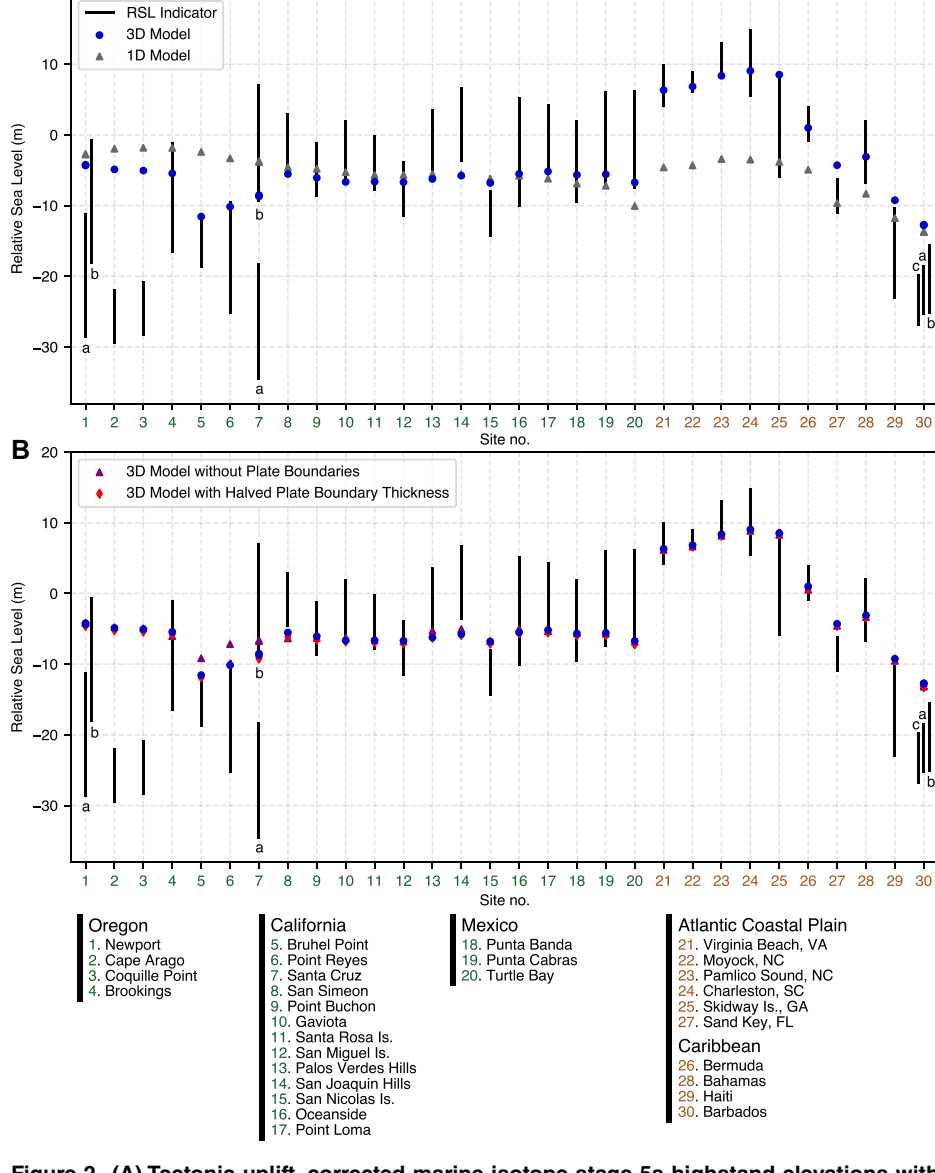


Figure 2. (A) Tectonic uplift–corrected marine isotope stage 5a highstand elevations with uncertainty (vertical bars) and glacial isostatic adjustment (GIA) predictions for North American Pacific and Atlantic-Caribbean coastal sites (Table S1 [see text footnote 1]). Predictions are distinguished by earth model in the GIA simulation: gray triangles, background one-dimensional (1-D) model; blue dots, three-dimensional (3-D) earth model (Fig. 1). (B) As in A with the 1-D predictions replaced by two 3-D predictions that remove plate boundaries or decrease (halve) the plate boundary thickness. a, b, and c labels refer to the relative sea level (RSL) indicator sub-sites referenced in Table S1. See Figure 1 for a key to U.S. state abbreviations.

subsidence of the peripheral bulge (Figs. 3A and 3C). This brings the present-day elevation of the bulge closer to the elevation during MIS 5a. For example, along the coast from Oregon to Baja California, the 3-D prediction varies by  $\sim 6$  m (Fig. 3A). These earth model changes also increase the shore-perpendicular gradient in the GIA signal by amplifying the response to ocean loading.

## DISCUSSION

Creveling et al. (2017) demonstrated that weakening the upper mantle viscosity in 1-D earth models to  $\sim 10^{20}$  Pa·s shifted the predicted North American peripheral bulge southward

such that most Pacific coast sites were positioned on the inner rather than outer flank of the peripheral bulge, reversing the north-south highstand elevation gradient predicted using an upper mantle viscosity of  $\sim 5 \times 10^{20}$  Pa·s. In the 3-D GIA simulation, the mean upper mantle viscosity below the Pacific coast is  $\sim 10^{20}$  Pa·s, but the reduced north-south gradient compared to the 1-D simulation arises from a reduced elevation difference between MIS 5a and present day rather than a change in the peripheral bulge position.

The large suite of 1-D earth models considered by Creveling et al. (2017), including the background 1-D model, was incapable of fit-

ting the MIS 5a highstand indicators to the level obtained in the 3-D GIA simulation. For our GIA prediction based on the 1-D background model, fits to observational data are poor along both coasts (Fig. 2A, gray triangles). While Atlantic and Caribbean RSL predictions follow the observed southward-decreasing trend in highstand elevations, the magnitude of this gradient is too small. The 1-D GIA model predicts a more muted variability in highstand elevations in northern California compared to that observed. The  $\chi^2$  misfit between all the predicted and observed Pacific and Atlantic-Caribbean highstand elevations are 5.05 and 12.59, respectively. In contrast, the introduction of lateral variations in mantle viscosity and lithospheric thickness reconcile the distinct geographic trends in MIS 5a highstand elevations between the North American Pacific and Atlantic-Caribbean coasts (Fig. 2A, blue dots). The steeper north-south gradient predicted by the 3-D GIA model for the Atlantic coast provides an excellent match to the data, with a peak-to-peak amplitude of  $\sim$ 20 m (Fig. 2A) and a  $\chi^2$  misfit of 2.03. This misfit drops to 1.42 when considering only one Barbados site (Cave Hill). (The 1-D prediction misfit increases to 14.39 with only Cave Hill.) The Pacific coast fit also improves, apart from several sites in Oregon where the predicted elevation is  $\sim$ 15–20 m higher than observed. The  $\chi^2$  misfit of the 3-D prediction to the observations at all Pacific coast sites is 3.46. This misfit drops to 0.99 when Oregon highstand data are omitted (The analogous Oregon-omitted  $\chi^2$ for the 1-D prediction is 1.89.) To explore the significance of this misfit, we perform a sensitivity study in which we compute highstand values at locations determined by shifting all sites 400 km north and 200 km east. The results (Fig. S1 in the Supplemental Material) indicate that predictions of highstand elevations at sites closest to MIS 5a ice cover are sensitive to their distance to the model ice sheet perimeter. Sites south of Oregon are significantly less sensitive to the ice perimeter. Shifting the model ice sheet southwest would perturb the predicted highstands downward at the Oregon coastal sites and improve the fit to these observations. Some of the misfit may also reflect inaccuracy in the 3-D structure of the model and/or tectonic uplift-corrected indicator elevations.

We explore the sensitivity of predictions to changes in the treatment of plate boundaries in the 3-D GIA model with simulations halving the width of the plate boundary zone and excluding plate boundaries (Fig. 2B). The predictions are insensitive to this reduction in plate boundary thickness and, except for northern California sites Bruhel Point, Point Reyes, and Santa Cruz, to removing the plate boundaries entirely. Figure S2 shows that this geographically limited sensitivity arises because the three sites are located within 10 km of the San Andreas fault, a dis-

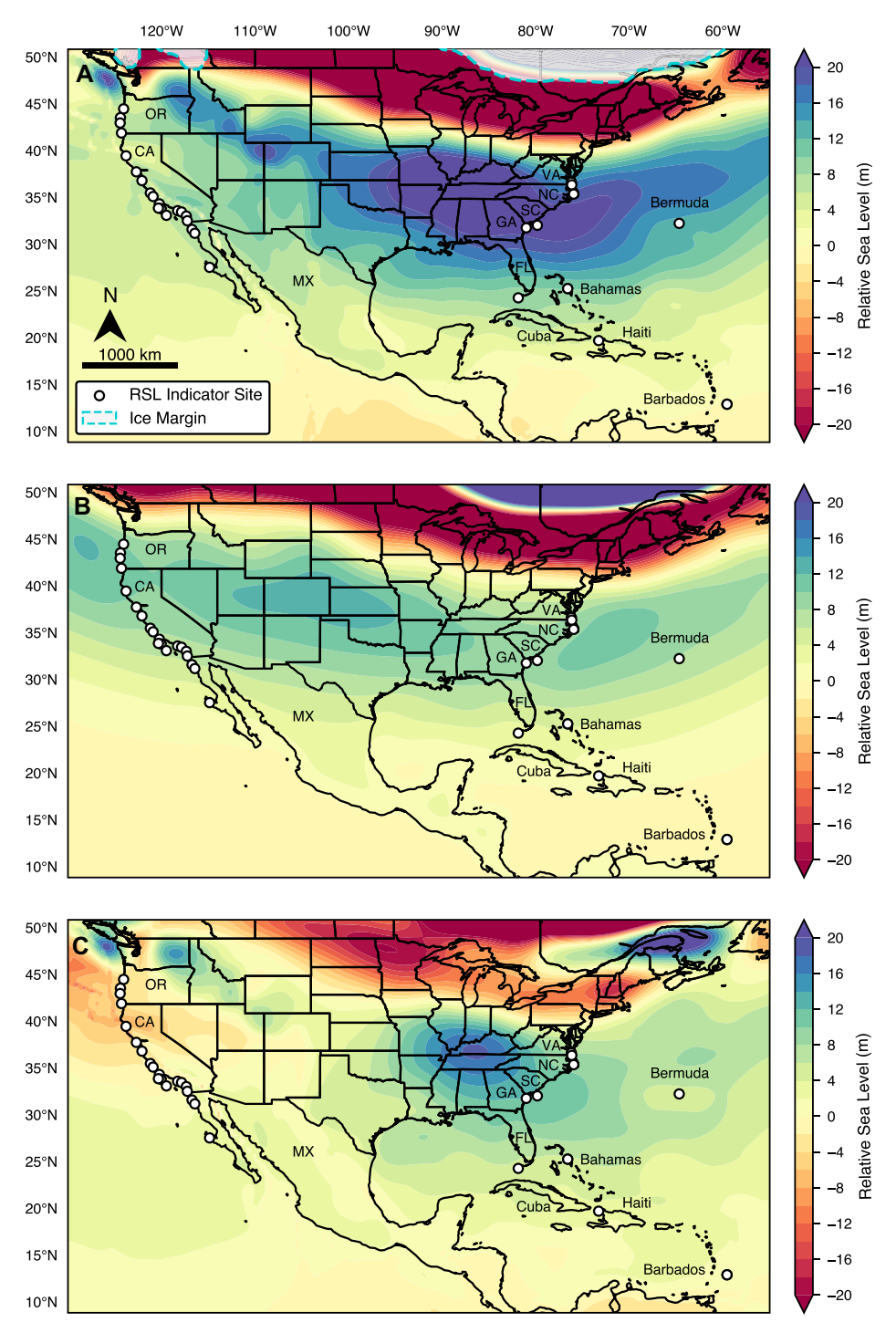


Figure 3. (A, B) Glacial isostatic adjustment prediction of marine isotope stage (MIS) 5a relative sea level (RSL) computed using the three-dimensional (3-D) (A) and background one-dimensional (1-D) (B) earth models. Both maps have the MIS 5a and present-day difference in global mean sea level (-13.0 m) removed from the total predicted signal. (C) Difference between the 3-D and 1-D predictions (panel A minus panel B). See Figure 1 for key.

tance well within the modeled thickness of the local lithosphere (Fig. 1A).

We repeated the 1-D background calculation with a PC2T ice history that modified the ice volume between MISs 5a and 5c, changing the MIS 5b (90 ka) GMSL value to -30 m from -40 m. We found that MIS 5a highstand predictions in Figure 2A (gray triangles) were shifted

relatively uniformly upward by  $\sim\!2$  m, suggesting that uncertainty in MIS 5b ice volume maps into a small yet discernable uncertainty in MIS 5a GMSL.

#### CONCLUSIONS

GIA modeling incorporating realistic 3-D viscoelastic earth structure can reconcile com-

plex regional patterns in peak MIS 5a RSL indicator elevations that could not previously be reproduced by a single 1-D GIA model. We emphasize that the fit of the 3-D GIA predictions is not statistically different from the fit achieved by Creveling et al. (2017) using GIA simulations based on distinct 1-D earth models for each coast. This reconciliation builds upon a new global model of ice history through the last glaciation (Pico et al., 2017; Creveling et al., 2017) and improved constraints on 3-D mantle viscoelastic structure (Richards et al., 2020; Hoggard et al., 2020; Austermann et al., 2021) based on high-resolution seismic tomography. Model fits are improved for the Atlantic coastline, yet the misfit of the 3-D predictions to Oregon highstand observations, a location with large differences between the 3-D and 1-D earth structure and sensitive to ice history, motivates a future comprehensive assessment of the uncertainties inherent in GIA studies (Melini and Spada, 2019).

The success of the 3-D earth model opens avenues for future refinement of MIS 5a peak GMSL. Estimates of MIS 5a peak GMSL based on 1-D GIA simulations have conflicted, ranging from -28 m when fitting North American Atlantic-Caribbean data (Potter and Lambeck, 2003) to -15.2 m using North American Pacific data (Simms et al., 2015). Creveling et al. (2017) inferred a bound on peak MIS 5a GMSL of  $-10.5 \pm 5.5$  m using GIA simulations based on independent 1-D earth models for the two regions. Our reconciliation of highstand data from both coasts using an ice history characterized by a peak MIS 5a GMSL of -13 m and a 3-D earth model consistent with a broad range of geophysical data supports the inferences of Simms et al. (2015) and Creveling et al. (2017) that net MIS 5a ice volume was closer to an interglacial state. Similar refinements of peak GMSL may be possible for other episodes of ice-age warmth preceding the Holocene epoch, such as for MIS 5c or the LIG (Kopp et al., 2009; Dyer et al., 2021) in which Austermann et al. (2021) detected the impact of lateral variations in mantle viscosity. Such analyses can yield refinements in model input such as ice history and improve quality assessments for sites with conflicting highstand elevations.

## ACKNOWLEDGMENTS

This research was made possible by National Science Foundation award 1927326 and benefited from conversation with Dan Muhs. We thank Jacky Austermann, Mark Hoggard, Fred Richards, and Tamara Pico for their construction of the earth and ice models adopted here. We thank editor Kathleen Benison and four anonymous reviewers for the constructive reviews that improved this contribution.

# REFERENCES CITED

Austermann, J., Mitrovica, J.X., Latychev, K., and Milne, G.A., 2013, Barbados-based estimate of ice volume at Last Glacial Maximum affected

- by subducted plate: Nature Geoscience, v. 6, p. 553–557, https://doi.org/10.1038/ngeo1859.
- Austermann, J., Hoggard, M.J., Latychev, K., Richards, F.D., and Mitrovica, J.X., 2021, The effect of lateral variations in Earth structure on Last Interglacial sea level: Geophysical Journal International, v. 227, p. 1938–1960, https://doi.org/10.1093/gji/ggab289.
- Burdick, S., Li, C., Martynov, V., Cox, T., Eakins, J., Mulder, T., Astiz, L., Vernon, F.L., Pavlis, G.L., and van der Hilst, R.D., 2008, Upper mantle heterogeneity beneath North America from travel time tomography with global and USArray transportable array data: Seismological Research Letters, v. 79, p. 384–392, https://doi.org/10.1785/ gssrl.79.3.384.
- Clark, J., Mitrovica, J.X., and Latychev, K., 2019, Glacial isostatic adjustment in central Cascadia: Insights from three-dimensional Earth modeling: Geology, v. 47, p. 295–298, https://doi.org /10.1130/G45566.1.
- Creveling, J.R., Mitrovica, J.X., Hay, C.C., Austermann, J., and Kopp, R.E., 2015, Revisiting tectonic corrections applied to Pleistocene sea-level highstands: Quaternary Science Reviews, v. 111, p. 72–80, https://doi.org/10.1016/j.quascirev.2015.01.003.
- Creveling, J.R., Mitrovica, J.X., Clark, P.U., Waelbroeck, C., and Pico, T., 2017, Predicted bounds on peak global mean sea level during marine isotope stages 5a and 5c: Quaternary Science Reviews, v. 163, p. 193–208, https://doi.org/10.1016/j.quascirev.2017.03.003.
- Cutler, K.B., Edwards, R.L., Taylor, F.W., Cheng, H., Adkins, J., Gallup, C.D., Cutler, P.M., Burr, G.S., and Bloom, A.L., 2003, Rapid sea-level fall and deep-ocean temperature change since the last interglacial period: Earth and Planetary Science Letters, v. 206, p. 253–271, https://doi.org/10 .1016/S0012-821X(02)01107-X.
- Dutton, A., Carlson, A.E., Long, A.J., Milne, G.A., Clark, P.U., DeConto, R., Horton, B.P., Rahmstorf, S., and Raymo, M.E., 2015, Sea-level rise due to polar ice-sheet mass loss during past warm periods: Science, v. 349, https://doi.org/10.1126/ science.aaa4019.
- Dyer, B., Austermann, J., D'Andrea, W.J., Creel, R.C., Sandstrom, M.R., Cashman, M., Rovere, A., and Raymo, M.E., 2021, Sea-level trends across the Bahamas constrain peak last interglacial ice melt: Proceedings of the National Academy of Sciences of the United States of America, v. 118, https://doi.org/10.1073/pnas.2026839118.
- Hoggard, M.J., Czarnota, K., Richards, F.D., Huston, D.L., Jaques, A.L., and Ghelichkhan, S., 2020, Global distribution of sediment-hosted metals controlled by craton edge stability: Nature Geoscience, v. 13, p. 504–510, https://doi.org/10 .1038/s41561-020-0593-2.
- James, T.S., Clague, J.J., Wang, K., and Hutchinson, I., 2000, Postglacial rebound at the northern Cascadia subduction zone: Quaternary Science Reviews, v. 19, p. 1527–1541, https://doi.org/10 .1016/S0277-3791(00)00076-7.

- Kendall, R.A., Mitrovica, J.X., and Milne, G.A., 2005, On post-glacial sea level—II. Numerical formulation and comparative results on spherically symmetric models: Geophysical Journal International, v. 161, p. 679–706, https://doi.org/10.1111/j.1365-246X.2005.02553.x.
- Kopp, R.E., Simons, F.J., Mitrovica, J.X., Maloof, A.C., and Oppenheimer, M., 2009, Probabilistic assessment of sea level during the last interglacial stage: Nature, v. 462, p. 863–867, https://doi.org/10.1038/nature08686.
- Kuchar, J., Milne, G., and Latychev, K., 2019, The importance of lateral Earth structure for North American glacial isostatic adjustment: Earth and Planetary Science Letters, v. 512, p. 236–245, https://doi.org/10.1016/j.epsl.2019.01.046.
- Lambeck, K., and Chappell, J., 2001, Sea level change through the last glacial cycle: Science, v. 292, p. 679–686, https://doi.org/10.1126/science.1059549.
- Lambeck, K., Rouby, H., Purcell, A., Sun, Y., and Sambridge, M., 2014, Sea level and global ice volumes from the Last Glacial Maximum to the Holocene: Proceedings of the National Academy of Sciences of the United States of America, v. 111, p. 15,296–15,303, https://doi.org/10.1073 /pnas.1411762111.
- Latychev, K., Mitrovica, J.X., Tromp, J., Tamisiea, M.E., Komatitsch, D., and Christara, C.C., 2005, Glacial isostatic adjustment on 3-D earth models: A finite-volume formulation: Geophysical Journal International, v. 161, p. 421–444, https://doi.org/10.1111/j.1365-246X.2005.02536.x.
- Lau, H.C.P., Mitrovica, J.X., Austermann, J., Crawford, O., Al-Attar, D., and Latychev, K., 2016, Inferences of mantle viscosity based on ice age data sets: Radial structure: Journal of Geophysical Research. Solid Earth, v. 121, p. 6991–7012, https://doi.org/10.1002/2016JB013043.
- Li, T., Wu, P., Steffen, H., and Wang, H., 2018, In search of laterally heterogeneous viscosity models of glacial isostatic adjustment with the ICE-6G\_C global ice history model: Geophysical Journal International, v. 214, p. 1191–1205, https://doi.org/10.1093/gji/ggy181.
- Li, T., Khan, N.S., Baranskaya, A.V., Shaw, T.A., Peltier, W.R., Stuhne, G.R., Wu, P., and Horton, B.P., 2022, Influence of 3D Earth structure on glacial isostatic adjustment in the Russian Arctic: Journal of Geophysical Research. Solid Earth, v. 127, https://doi.org/10.1029/2021JB023631.
- Melini, D., and Spada, G., 2019, Some remarks on Glacial Isostatic Adjustment modelling uncertainties: Geophysical Journal International, v. 218, p. 401–413, https://doi.org/10.1093/gji/ggz158.
- Mitrovica, J.X., and Milne, G.A., 2003, On post-glacial sea level: I. General theory: Geophysical Journal International, v. 154, p. 253–267, https://doi.org/10.1046/j.1365-246X.2003.01942.x.
- Mitrovica, J.X., Wahr, J., Matsuyama, I., and Paulson, A., 2005, The rotational stability of an ice-age earth: Geophysical Journal International, v. 161, p. 491–506, https://doi.org/10.1111/j.1365-246X.2005.02609.x.

- Nield, G.A., Whitehouse, P.L., van der Wal, W., Blank, B., O'Donnell, J.P., and Stuart, G.W., 2018, The impact of lateral variations in lithospheric thickness on glacial isostatic adjustment in West Antarctica: Geophysical Journal International, v. 214, p. 811–824, https://doi.org/10 .1093/gji/ggy158.
- Peltier, W.R., Argus, D.F., and Drummond, R., 2015, Space geodesy constrains ice age terminal deglaciation: The ICE-6G\_C (VM5a) model: Journal of Geophysical Research: Solid Earth, v. 120, p. 450–487, https://doi.org/10.1002 /2014JB011176.
- Pico, T., Creveling, J.R., and Mitrovica, J.X., 2017, Sea-level records from the U.S. mid-Atlantic constrain Laurentide Ice Sheet extent during Marine Isotope Stage 3: Nature Communications, v. 8, https://doi.org/10.1038/ncomms15612.
- Potter, E.K., and Lambeck, K., 2003, Reconciliation of sea-level observations in the Western North Atlantic during the last glacial cycle: Earth and Planetary Science Letters, v. 217, p. 171–181, https://doi.org/10.1016/S0012-821X(03)00587-9.
- Powell, E.M., Pan, L., Hoggard, M.J., Latychev, K., Gomez, N., Austermann, J., and Mitrovica, J.X., 2021, The impact of 3-D Earth structure on farfield sea level following interglacial West Antarctic Ice Sheet collapse: Quaternary Science Reviews, v. 273, https://doi.org/10.1016/j.quascirev .2021.107256.
- Richards, F.D., Hoggard, M.J., White, N., and Ghelichkhan, S., 2020, Quantifying the relationship between short-wavelength dynamic topography and thermomechanical structure of the upper mantle using calibrated parameterization of anelasticity: Journal of Geophysical Research: Solid Earth, v. 125, https://doi.org/10.1029/2019JB019062.
- Schaeffer, A.J., and Lebedev, S., 2014, Imaging the North American continent using waveform inversion of global and USArray data: Earth and Planetary Science Letters, v. 402, p. 26–41, https:// doi.org/10.1016/j.epsl.2014.05.014.
- Simms, A.R., Rouby, H., and Lambeck, K., 2015, Marine terraces and rates of vertical tectonic motion: The importance of glacio-isostatic adjustment along the Pacific coast of central North America: Geological Society of America Bulletin, v. 128, p. 81–93, https://doi.org/10.1130/B31299.1.
- Wu, P., and van der Wal, W., 2003, Postglacial sealevels on a spherical, self-gravitating viscoelastic earth: Effects of lateral viscosity variations in the upper mantle on the inference of viscosity contrasts in the lower mantle: Earth and Planetary Science Letters, v. 211, p. 57–68, https://doi.org/10.1016/S0012-821X(03)00199-7.
- Zhong, S., Paulson, A., and Wahr, J., 2003, Threedimensional finite-element modelling of Earth's viscoelastic deformation: Effects of lateral variations in lithospheric thickness: Geophysical Journal International, v. 155, p. 679–695, https://doi .org/10.1046/j.1365-246X.2003.02084.x.

Printed in USA